A Sparse Bayesian Learning Based Joint Channel and Impulsive Noise Estimation Algorithm for Underwater Acoustic OFDM Systems

Shuche Wang*, Zhiqiang He*,♭, Kai Niu*, Peng Chen†, and Yue Rong†
*Key Laboratory of Universal Wireless Communications, Ministry of Education,
Beijing University of Posts and Telecommunications (BUPT), Beijing, China
♭Key Laboratory of Underwater Acoustic Communication and Marine Information Technology, Ministry of Education,
Xiamen University, Xiamen, China
†School of Electrical Engineering, Computing and Mathematical Sciences, Curtin University, Bentley, WA 6102, Australia

***Abstract*—Impulsive noise can significantly affect the performance of underwater acoustic (UA) orthogonal frequency-division multiplexing (OFDM) systems. In this paper, by utilizing the pilot subcarriers, we propose a novel sparse Bayesian learning based expectation maximization algorithm for joint channel estimation and impulsive noise mitigation in UA OFDM systems. Moreover, an adaptive clipping threshold method together with a minimum mean-squared error estimator are developed to improve the estimation of the positions and amplitudes of impulsive noise. The performance of the proposed algorithm is verified both through numerical simulations and by data collected during a UA communication experiment conducted in December 2015 in the estuary of the Swan River, Western Australia. The results show that the proposed algorithm is more effective in mitigating impulsive noise than existing methods.**

***Index Terms*—Underwater acoustic communication, OFDM, Impulsive noise, Sparse Bayesian learning.**

I. Introduction

It is well known that underwater acoustic (UA) channel is one of the most challenging channels for wireless communication because of extremely limited bandwidth, severe fading, strong multipath interference, and significant Doppler shifts [1]. In the past decades, the orthogonal frequency-division multiplexing (OFDM) technology has been applied to mitigate the inter-symbol interference (ISI) in high-rate underwater acoustic communication systems [2]. However, impulsive noise introduced by nature sources and human activities can significantly degrade the performance of UA OFDM systems [3], [4]. Thus, it is essential to estimate and mitigate impulsive noise in UA communication systems.

One class of impulsive noise mitigation methods first find the impulsive noise positions by threshold testing and then use blanking or clipping methods to adjust impulsive noise dominated samples [5]. However, these methods may destroy the received signals. Moreover, a fixed threshold is usually used in these methods which is not adaptive to time-varying received signals and noise. Another class of impulsive noise mitigation techniques exploit the sparsity of impulsive noise and the structure of OFDM signals [6]-[10]. Recently, a joint channel estimation and impulsive noise mitigation method has been proposed in [11], which has an improved performance compared with traditional least-squares (LS) based channel estimation methods and blanking based impulsive noise mitigation approaches.

In this paper, considering the sparsity of channel impulse response and the impulsive noise of UA channels, we propose a sparse Bayesian learning (SBL) [12]-[14] based expectation maximization (EM) algorithm to jointly estimate the channel impulse response and the impulsive noise by utilizing the received signals at the pilot subcarriers. Moreover, compared with traditional fixed threshold testing methods, an adaptive clipping threshold method [15] is applied to further improve the accuracy in estimating the positions of impulsive noise.

The proposed algorithm is evaluated and compared with existing methods through numerical simulations and by real data collected during a UA communication experiment conducted in December 2015 in the estuary of the Swan River, Western Australia. Both simulation and experiment results show that compared with existing methods, the proposed algorithm is more effective in mitigating impulsive noise in UA OFDM systems than existing methods, and achieves an improved system bit-error-rate (BER) and frame-error-rate (FER) performance.

II. System model

We consider a frame based coded OFDM system with N_c subcarriers [11], which contains N_s subcarriers for data transmission, N_p uniformly spaced pilot subcarriers and N_u null subcarriers at each edge of the passband. In each frame, an L_b long binary source data stream $\mathbf{b}$ is encoded, interleaved, and punctured to form a coded sequence $\mathbf{c}$ with a length of $L_c = R_m N_s N_b$, where R_m is the modulation order and N_b denotes the number of OFDM blocks in one frame. Then the coded sequence $\mathbf{c}$ is mapped into $N_s N_b$ data symbols by the phase-shift keying (PSK) or quadrature amplitude modulation (QAM) constellations.

Through the inverse discrete Fourier transform (IDFT), the baseband signal in the time domain of one OFDM symbol can be expressed as

$$\mathbf{x} = \mathbf{F}^H \mathbf{d} \tag{1}$$

where $(\cdot)^H$ stands for Hermitian transpose, $\mathbf{F}$ is an $N_c \times N_c$ normalized DFT matrix, and $\mathbf{d}$ is the transmitted OFDM symbol vector. To prevent ISI caused by multipath fading, the transmitter then inserts the cyclic prefix (CP) with a length of T_{cp} in front of each OFDM symbol. We assume that the subcarrier spacing is f_{sc}. Thus, the bandwidth of the transmitted signal is $B = f_{sc}N_c$, the duration of one OFDM symbol is $T = 1/f_{sc}$, and the total length of one OFDM block is $T_{total} = T + T_{cp}$.

After the frequency offset compensation, downshifting, low-pass filtering, sampling, and removing the cyclic prefix, the time domain and frequency domain received signal vectors can be written as

$$\mathbf{r}_t = \mathbf{F}^H\mathbf{D}\mathbf{F}\mathbf{h}_t + \mathbf{v}_t + \mathbf{w}_t \tag{2}$$

$$\mathbf{r}_f = \mathbf{D}\mathbf{h}_f + \mathbf{v}_f + \mathbf{w}_f \tag{3}$$

where $\mathbf{D} = \mathrm{diag}(\mathbf{d})$ is a diagonal matrix taking $\mathbf{d}$ as the main diagonal elements, $\mathbf{v}_t$ and $\mathbf{w}_t$ are the time domain impulsive noise and the background Gaussian noise vectors, respectively, $\mathbf{h}_t$ denotes the time domain channel impulse response, $\mathbf{h}_f = \mathbf{F}\mathbf{h}_t$, $\mathbf{v}_f = \mathbf{F}\mathbf{v}_t$, and $\mathbf{w}_f = \mathbf{F}\mathbf{w}_t$.

III. The Proposed Approach

In this section, we propose an SBL based joint channel and impulsive noise estimation algorithm, where the estimation of the channel impulse response and impulsive noise is converted to solving an under-determined linear regression problem under sparsity constraints. Compared with various compressed sensing algorithms, sparse Bayesian learning has attracted increasing attention due to its improved robustness over greedy algorithms such as the orthogonal matching pursuit (OMP).

Let us introduce an $N_p \times N_c$ matrix $\mathbf{P}$ which selects N_p pilot subcarriers out of total N_c subcarriers. From (3), the received signal vector at the pilot subcarriers is given by

$$\mathbf{r}_p = \mathbf{D}_p\mathbf{h}_p + \mathbf{v}_p + \mathbf{w}_p \tag{4}$$

where $\mathbf{D}_p = \mathrm{diag}(\mathbf{d}_p)$, $\mathbf{d}_p$ is the pilot sequence, $\mathbf{h}_p$ contains the channel frequency response at pilot subcarriers, $\mathbf{v}_p = \mathbf{P}\mathbf{v}_f$, and $\mathbf{w}_p = \mathbf{P}\mathbf{w}_f$.

By introducing $\mathbf{h}_{p,t} = \mathbf{F}_p^H\mathbf{h}_p$ and $\mathbf{v}_{p,t} = \mathbf{F}_p^H\mathbf{v}_p$, where $\mathbf{F}_p$ is an $N_p \times N_p$ DFT matrix, (4) can be rewritten as

$$\begin{aligned}\mathbf{r}_p &= \mathbf{D}_p\mathbf{F}_p\mathbf{h}_{p,t} + \mathbf{F}_p\mathbf{v}_{p,t} + \mathbf{w}_p \\ &= \mathbf{M}\boldsymbol{\theta} + \mathbf{w}_p \end{aligned} \tag{5}$$

where $\mathbf{M} = (\mathbf{D}_p\mathbf{F}_p, \mathbf{F}_p)$, $\boldsymbol{\theta} = (\mathbf{h}_{p,t}^T, \mathbf{v}_{p,t}^T)^T$, and $(\cdot)^T$ denotes transpose. Since $\mathbf{w}_p$ is Gaussian, $\boldsymbol{\theta}$ can be estimated from (5) using the LS method [11]. However, as the UA channel is sparse, only a few entries of $\mathbf{h}_{p,t}$ are non-zero, and $\mathbf{v}_{p,t}$ can be viewed as a 'fold-and-add' version of $\mathbf{v}$ which can be considered to be sparse as well. Thus, $\boldsymbol{\theta}$ is a sparse vector. In this case, the LS estimator may result in over-fitting. To solve this issue and improve the accuracy of estimation, we apply the SBL method by considering the sparsity of $\boldsymbol{\theta}$.

We assume that $\mathbf{w}_p$ has independent and identically distributed complex Gaussian entries with zero mean and variance β^{-1}. Thus, the likelihood of (5) can be written as

$$p(\mathbf{r}_p|\boldsymbol{\theta}, \beta) = (\beta/\pi)^{N_p} \exp(-\beta\|\mathbf{r}_p - \mathbf{M}\boldsymbol{\theta}\|^2) \tag{6}$$

where $\|\cdot\|$ denotes the Euclidean norm of a vector. To avoid over-fitting, we assume that $\boldsymbol{\theta}$ has a complex Gaussian prior distribution with zero mean and variance α_i^{-1} for its ith entry as

$$p(\boldsymbol{\theta}|\boldsymbol{\alpha}) = \pi^{-N_p} \prod_{i=1}^{N_p} \alpha_i \exp(-\boldsymbol{\theta}^H \mathrm{diag}(\boldsymbol{\alpha})\boldsymbol{\theta}) \tag{7}$$

where $\boldsymbol{\alpha} = [\alpha_1, \ldots, \alpha_{N_p}]^T$. To avoid over-parameterization, we treat the parameters $\boldsymbol{\alpha}$ and β as random variables

$$p(\boldsymbol{\alpha}) = \prod_{i=1}^{N_p} \gamma(\alpha_i; a, b), \quad p(\beta) = \gamma(\beta; c, d) \tag{8}$$

where $\gamma(\cdot)$ denotes the Gamma distribution and a, b, c, d are parameters of the Gamma distributions.

The estimation of $\boldsymbol{\theta}$ requires the calculation of the posterior distribution, which from the Bayes' rule is given by

$$p(\boldsymbol{\theta}, \boldsymbol{\alpha}, \beta|\mathbf{r}_p) = \frac{p(\mathbf{r}_p|\boldsymbol{\theta}, \boldsymbol{\alpha}, \beta)p(\boldsymbol{\theta}, \boldsymbol{\alpha}, \beta)}{p(\mathbf{r}_p)} \tag{9}$$

where $p(\mathbf{r}_p) = \int p(\mathbf{r}_p|\boldsymbol{\theta}, \boldsymbol{\alpha}, \beta)p(\boldsymbol{\theta}, \boldsymbol{\alpha}, \beta)\, d\boldsymbol{\theta} d\boldsymbol{\alpha} d\beta$ cannot be directly calculated. Interestingly, $p(\boldsymbol{\theta}, \boldsymbol{\alpha}, \beta|\mathbf{r}_p)$ can be decomposed as

$$p(\boldsymbol{\theta}, \boldsymbol{\alpha}, \beta|\mathbf{r}_p) = p(\boldsymbol{\theta}|\mathbf{r}_p, \boldsymbol{\alpha}, \beta)p(\boldsymbol{\alpha}, \beta|\mathbf{r}_p). \tag{10}$$

where

$$p(\boldsymbol{\theta}|\mathbf{r}_p, \boldsymbol{\alpha}, \beta) = \frac{p(\mathbf{r}_p|\boldsymbol{\theta}, \beta)p(\boldsymbol{\theta}|\boldsymbol{\alpha})}{p(\mathbf{r}_p|\boldsymbol{\alpha}, \beta)} = \frac{p(\mathbf{r}_p|\boldsymbol{\theta}, \beta)p(\boldsymbol{\theta}|\boldsymbol{\alpha})}{\int p(\mathbf{r}_p|\boldsymbol{\theta}, \beta)p(\boldsymbol{\theta}|\boldsymbol{\alpha})\, d\boldsymbol{\theta}}. \tag{11}$$

Note that the numerator of (11) is the product of two Gaussian density functions and the denominator of (11) is the convolution of them. From (6) and (7), we have

$$p(\boldsymbol{\theta}|\mathbf{r}_p, \boldsymbol{\alpha}, \beta) = \pi^{-N_p}|\boldsymbol{\Sigma}|^{-1} \exp(-(\boldsymbol{\theta}-\boldsymbol{\mu})^H\boldsymbol{\Sigma}^{-1}(\boldsymbol{\theta}-\boldsymbol{\mu})) \tag{12}$$

where $(\cdot)^{-1}$ and $|\cdot|^{-1}$ denote matrix inversion and determinant, respectively, and

$$\boldsymbol{\Sigma} = (\beta\mathbf{M}^H\mathbf{M} + \mathrm{diag}(\boldsymbol{\alpha}))^{-1} \qquad \boldsymbol{\mu} = \beta\boldsymbol{\Sigma}\mathbf{M}^H\mathbf{r}_p. \tag{13}$$

Based on (12), the optimal $\boldsymbol{\theta}$ is given by

$$\boldsymbol{\theta} = \boldsymbol{\mu} \tag{14}$$

which depends on $\boldsymbol{\alpha}$ and β as seen from (13).

The optimal $\boldsymbol{\alpha}$ and β are obtained by maximizing $p(\boldsymbol{\alpha}, \beta|\mathbf{r}_p)$ in (10). However, $p(\boldsymbol{\alpha}, \beta|\mathbf{r}_p)$ cannot be expressed in analytic form. To solve this issue, we apply the EM algorithm as follows. From (6)-(8), we obtain the log-likelihood function as

$$\mathcal{L} = \ln(p(\mathbf{r}_p|\boldsymbol{\theta}, \beta)p(\boldsymbol{\theta}|\boldsymbol{\alpha})p(\boldsymbol{\alpha})p(\beta)). \tag{15}$$

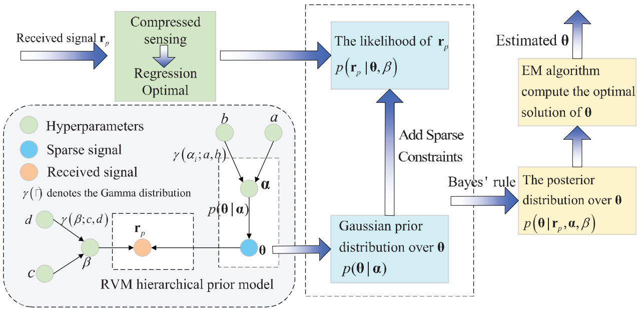

Fig. 1. Block diagram of the proposed SBL estimation algorithm.

By ignoring the terms in (15) that are independent of $\boldsymbol{\alpha}$, we can obtain the optimal $\boldsymbol{\alpha}$ by maximizing

$$E_{p(\boldsymbol{\theta}|\boldsymbol{r}_p,\boldsymbol{\alpha},\beta)}[\ln(p(\boldsymbol{\theta}|\boldsymbol{\alpha})p(\boldsymbol{\alpha}))] \tag{16}$$

where $E_{p(\boldsymbol{\theta}|\boldsymbol{r}_p,\boldsymbol{\alpha},\beta)}[\cdot]$ stands for the expectation with respect to the distribution in (12). By setting the derivative of (16) with respect to α_i to zero, we obtain

$$\alpha_i = \frac{a+1}{b+\sigma_{i,i}+|\mu_i|^2}, \quad i=1,\ldots,N_p \tag{17}$$

where $\sigma_{i,i}$ and μ_i denote the (i,i)-th element of $\boldsymbol{\Sigma}$ and the ith element of $\boldsymbol{\mu}$ in (13), respectively. Similarly, β can be optimized by maximizing $E_{p(\boldsymbol{\theta}|\boldsymbol{r}_p,\boldsymbol{\alpha},\beta)}[\ln(p(\mathbf{r}_p|\boldsymbol{\theta},\beta)p(\beta))]$, leading to

$$\beta = (c+N_p)/\tilde{d} \tag{18}$$

where $\tilde{d} = d + \mathbf{r}_p^H\mathbf{r}_p - \mathbf{r}_p^H\mathbf{M}\boldsymbol{\mu} - \boldsymbol{\mu}^H\mathbf{M}^H\mathbf{r}_p + \mathrm{tr}(\mathbf{M}\boldsymbol{\Sigma}\mathbf{M}^H) + \boldsymbol{\mu}^H\mathbf{M}^H\mathbf{M}\boldsymbol{\mu}$ and $\mathrm{tr}(\cdot)$ denotes the matrix trace. We update $\boldsymbol{\Sigma}$, $\boldsymbol{\mu}$, $\boldsymbol{\alpha}$, and β iteratively following (13), (17), and (18). After the convergence of the algorithm, the sparse $\boldsymbol{\theta}$ is obtained as (14). The procedure of the proposed SBL-EM estimation algorithm is shown in Fig. 1.

In order to use $\mathbf{v}_{p,t}$ (5) estimated from the SBL-EM algorithm above to obtain an estimation of $\mathbf{v}_t$ in (2), the positions of the impulsive noise also need to be known. Towards this end, we utilize a threshold test to collect the positions of possible impulsive noise in (2) into a set $\mathcal{I}_I$ which satisfies

$$|r_t(\mathcal{I}_I(i))|^2 > G\eta, \quad i=1,\ldots,N_I \tag{19}$$

where G is the average power of the received signal, N_I is the number of possible impulsive noise, and a constant threshold η is chosen in many existing works.

To improve the accuracy of estimating the impulsive noise positions, in this paper we apply an adaptive thresholding method which relies on the energy of the signal and noise and is given by [15]

$$\eta = \sqrt{\frac{2\sigma_a^2\sigma_b^2}{\sigma_b^2-\sigma_a^2}\ln\left(\frac{\sigma_a}{\sigma_b}\right)} \tag{20}$$

where $\sigma_a^2 = \sigma_s^2 + \sigma_w^2$, $\sigma_b^2 = \sigma_a^2 + \sigma_i^2$, σ_s^2, σ_w^2, and σ_i^2 are the variances of the signal, the Gaussian noise, and the impulsive noise, respectively. In practice, σ_a and σ_b can be estimated from (2) according to [15].

Let us introduce $\mathbf{v}_I$ as a vector which contains all the N_I samples of impulsive noise in one OFDM block. Thus, the impact of $\mathbf{v}_I$ on the N_p pilot subcarriers can be written as

$$\mathbf{v}_p = \mathbf{P}\mathbf{F}\boldsymbol{\Delta}\mathbf{v}_I \tag{21}$$

where $\boldsymbol{\Delta}$ is an $N_c \times N_I$ matrix indicating the position of the impulsive noise given by

$$\delta_{i,k} = \begin{cases} 1, & i=\mathcal{I}_I(k), k=1,\ldots,N_I \\ 0, & \text{otherwise.} \end{cases} \tag{22}$$

After the positions of impulsive noise are obtained, a minimum mean-squared error (MMSE) estimator is applied to estimate $\mathbf{v}_I$ as

$$\hat{\mathbf{v}}_I = (\mathbf{F}_I\mathbf{F}_I^H + (\sigma_w^2/\sigma_i^2)\mathbf{I}_{N_I})^{-1}\mathbf{F}_I^H\mathbf{F}_p\hat{\mathbf{v}}_{p,t} \tag{23}$$

where $\mathbf{I}_{N_I}$ is the $N_I \times N_I$ identity matrix, $\mathbf{F}_I = \mathbf{P}\mathbf{F}\boldsymbol{\Delta}$, and $\hat{\mathbf{v}}_{p,t}$ is the estimated $\mathbf{v}_{p,t}$.

IV. Simulation Results

In this section, we study the performance of the proposed algorithm through numerical simulations. In the simulations, the UA OFDM system has 512 subcarriers, which contains 325 data subcarriers, 128 pilot subcarriers for channel estimation, and 59 null subcarriers. The data symbols are modulated by 1/3 rate turbo encoded QPSK constellations, while the pilot symbols are modulated by QPSK constellations. Considering the code puncturing, the number of information-carrying bits in each frame is $L_b = 1088$. Thus the system source data rate is

$$R_b = \frac{L_b}{(T+T_{cp})(N_b+1)} = 1.19\text{kb/s}. \tag{24}$$

The multipath channel assumed in the simulation consists of 15 discrete paths, where the time delay between two adjacent paths follows the exponential distribution with a mean value of 1 ms. The phase of each path follows a uniform distribution between $-\pi$ and π and remains constant for each channel realization. The amplitudes of the paths are Rayleigh distributed with variances following an exponentially decreasing profile. The ratio of the channel variances between the start and the end of the CP is 20dB. We introduce $\mathbf{u} = \mathbf{v}_t + \mathbf{w}_t$ as the composite noise in (2). A Gaussian mixture model [10] is used to generate the composite noise with a probability density function (pdf) of

$$f(u_i) = \sum_{k=1}^{K} q_k\mathcal{N}(0,\sigma_k^2), \quad i=1,\cdots,N_c \tag{25}$$

where $\mathcal{N}(0,\sigma_k^2)$ denotes a complex Gaussian pdf with zero mean and variance σ_k^2, and q_k is the mixing probability of the k-th Gaussian component with $\sum_{k=1}^{K} q_k = 1$. In the simulations, similar to [16], we choose $K=2$, $q_1 = 0.98$, $q_2 = 0.02$, $\sigma_1^2 = \sigma_w^2$, and $\sigma_2^2 = \sigma_i^2$. The signal-to-noise ratio (SNR) is defined as $\mathrm{SNR} = \sigma_s^2/\sigma_w^2$, and the impulsive noise to background noise ratio is defined as $\mathrm{INR} = \sigma_i^2/\sigma_w^2$.

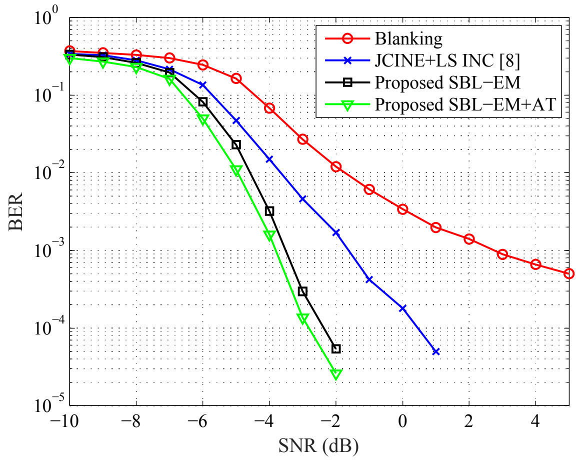

Fig. 2. BER performance of various algorithms versus SNR.

The BER of the proposed SBL-EM algorithm, the conventional blanking algorithm, and the JCINE+LS INC algorithm in [11] is shown in Fig. 2 versus the SNR with INR=26dB, where AT means adaptive threshold. It can be observed that the proposed SBL-EM algorithm has a gain of approximately 3dB compared with the JCINE+LS INC algorithm at high SNRs. Moreover, we can see from Fig. 2 that the adaptive threshold can further improve the system BER performance.

V. Experiment Results and Discussions

In this section, the proposed algorithm is applied to process the data recorded during a UA communication experiment conducted in December 2015 in the estuary of the Swan River, Western Australia. The locations of the transmitter and receiver was 936 meters as shown in Fig. 3. Both the transmitter transducer and the receiver hydrophone were mounted above the river bed on steel frames and were cabled to shore so that we can ignore the Doppler shift of the channel during the experiment. As the receiver hydrophone was located in warm shallow water close to a jetty, there was a significant amount of highly impulsive snapping shrimp noise. Another source of impulsive noise during the experiment was from waves breaking at the jetty piers whose intensity increases with the wind speed.

Key parameters of the experimental system are summarized in Table I. Similar to the numerical simulations, the pilot symbols are modulated by QPSK constellations. The data symbols are modulated by QPSK constellations encoded by either 1/2 or 1/3 rate turbo codes. Each transmission contains 500 frames with 250 frames for each coding rate. The data files recorded at the receiver during three transmissions were named T83, T84, and T85, respectively.

The proposed algorithm is applied to process the received data. The performance of the following impulsive noise estimation and mitigation algorithms are compared in Tables II-IV for the T83, T84, and T85 files, respectively.

Fig. 3. Transmitter and receiver locations during the experiment.

TABLE I
EXPERIMENTAL SYSTEM PARAMETERS

Number of OFDM blocks	N_b	5
Bandwidth	B	4 kHz
Carrier frequency	f_c	12 kHz
Sampling rate	f_s	96 kHz
Subcarrier spacing	f_{sc}	7.8 Hz
Length of OFDM symbol	T	128 ms
Length of CP	T_{cp}	25 ms

- LS channel estimator after blanking of the impulsive noise samples detected at the position of $\mathcal{I}_I$.
- JCINE algorithm with the LS based INC [11].
- Proposed SBL-EM algorithm.
- Proposed SBL-EM algorithm with adaptive threshold.

It can be seen from the results in Table II that since the signals in the T83 files are only slightly affected by impulsive noise, all four algorithms are able to obtain zero coded BER and FER. Moreover, the proposed SBL-EM and adaptive threshold algorithms yield a lower raw BER than existing methods.

As the signals in the T84 file are severely affected by impulsive noise, it can be seen from Table III that the existing LS+blanking and JCINE+LS INC algorithms have a very high FER with the 1/2 coding rate signals. However, the proposed algorithm has around 2% reduction in the raw BER, 7% reduction in the coded BER, and 35% reduction in the FER for the 1/2 coding rate signals. Moreover, for the 1/3 coding rate signals, the proposed algorithm reduces the FER from 4.1%

TABLE II
PERFORMANCE COMPARISON FOR THE T83 FILE

Coding rate	Method	Raw BER	Coded BER	FER
1/3	LS+blanking	5.2%	0	0
	JCINE+LS INC	3.5%	0	0
	SBL-EM	1.8%	0	0
	SBL-EM+AT	1.6%	0	0
1/2	LS+blanking	4.7%	0	0
	JCINE+LS INC	3.3%	0	0
	SBL-EM	1.9%	0	0
	SBL-EM+AT	1.6%	0	0

TABLE III
PERFORMANCE COMPARISON FOR THE T84 FILE

Coding rate	Method	Raw BER	Coded BER	FER
1/3	LS+blanking	15.5%	1.3%	7.3%
	JCINE+LS INC	14.7%	0.5%	4.1%
	SBL-EM	11.9%	0.07%	0.4%
	SBL-EM+AT	11.6%	0.04%	0.4%
1/2	LS+blanking	14.6%	15.9%	84.7%
	JCINE+LS INC	13.5%	11.1%	62.9%
	SBL-EM	11.4%	3.9%	27.7%
	SBL-EM+AT	11.1%	3.4%	23.1%

TABLE IV
PERFORMANCE COMPARISON FOR THE T85 FILE

Coding rate	Method	Raw BER	Coded BER	FER
1/3	LS+blanking	11.2%	0	0
	JCINE+LS INC	9.1%	0	0
	SBL-EM	5.6%	0	0
	SBL-EM+AT	5.3%	0	0
1/2	LS+blanking	11.7%	3.9%	24.8%
	JCINE+LS INC	9.8%	0.5%	5.2%
	SBL-EM	6.8%	0.2%	1.8%
	SBL-EM+AT	6.5%	0.1%	1.4%

to 0.4%.

As the signals in the T85 file suffer from middle level impulsive noise, it can be seen from Table IV that for the 1/3 coding rate signals, all four algorithms can obtain zero coded BER and FER. For the 1/2 coding rate signals, the proposed algorithm introduces around 3% decrease in the raw BER and FER. From Tables II- IV, we can conclude that the proposed algorithm has a better performance than existing methods.

VI. CONCLUSION

We have proposed a novel algorithm for improving the performance of UA OFDM systems in the presence of impulsive noise. To estimate and mitigate impulsive noise, we have developed an SBL-EM algorithm together with adaptive threshold for joint channel and impulsive noise estimation from the received signals. We have verified the performance of the proposed algorithms through numerical simulations and by data collected during a UA communication experiment. Compared with existing methods, the proposed algorithm can significantly improve the performance of UA OFDM systems under various environments.

VII. ACKNOWLEDGEMENT

This research was supported by the Australian Research Council's Discovery Projects funding scheme (DP140102131).

REFERENCES

[1] D. B. Kilfoyle and A. B. Baggeroer, "The state of the art in underwater acoustic telemetry," *IEEE J. Oceanic Engineering*, vol. 25, pp. 4-27, Jan. 2000.

[2] M. Stojanovic, "Low complexity OFDM detector for underwater acoustic channels," in *Proc. MTS/IEEE OCEANS*, Boston, USA, Sep. 2006.

[3] J. Hildebrand, "Anthropogenic and natural sources of ambient noise in the ocean," *Marine Ecol. Progr. Ser.*, vol. 395, pp. 5-20, Dec. 2009.

[4] M. Chitre, S. Kuselan, and V. Pallayil, "Ambient noise imaging in warm shallow waters; robust statistical algorithms and range estimation," *J. Acoustical Society of America*, vol. 132, no. 2, pp. 838-847, Aug. 2012.

[5] T. Suzuki, H. M. Tran, and T. Wada, "An underwater acoustic OFDM communication system with shrimp (impulsive) noise cancelling," in *Proc.MTS/IEEE OCEANS*, Washington, DC, Sep. 2005, vol. 2, pp. 996-1001.

[6] M. Chitre, J. R. Potter, and S. H. Ong, "Optimal and near-optimal signal detection in snapping shrimp dominated ambient noise," *IEEE J. Oceanic Engineering*, vol. 31, no. 2, pp. 497-503, Apr. 2006.

[7] H. Sun, W. Shen, Z. Wang, S. Zhou, X. Xu, and Y. Chen, "Joint carrier frequency offset and impulse noise estimation for underwater acoustic OFDM with null subcarriers," in *Proc. MTS/IEEE OCEANS*, Hampton Roads, VA, USA, Oct. 2012, pp. 14.

[8] P. Chen, Y. Rong, S. Nordholm, A. Duncan, and Z. He, "Compressed sensing based channel estimation and impulsive noise cancelation in underwater acoustic OFDM systems," in *Proc. IEEE TENCON*, Singapore, Nov. 22-25, 2016, pp. 2541-2544.

[9] P. Chen, Y. Rong, and S. Nordholm, "Pilot-subcarrier based impulsive noise mitigation for underwater acoustic OFDM systems," in *Proc. WUWNet 2016*, Shanghai, China, Oct. 24-26, 2016.

[10] X. Kuai, H. Sun, S. Zhou, and E. Chen, "Impulsive noise mitigation in underwater acoustic OFDM systems," *IEEE Trans. Veh. Technol.*, vol. 65, no. 10, pp. 8190-8202, Oct. 2016.

[11] P. Chen, Y. Rong, S. Nordholm, Z. He, and A. Duncan, "Joint channel estimation and impulsive noise mitigation in underwater acoustic OFDM communication systems," *IEEE Trans. Wireless Commun.*, vol. 16, pp. 6165-6178, Sep. 2017.

[12] M. E. Tipping, "Sparse Bayesian learning and the relevance vector machine," *J. Machine Learning Research*, vol. 1, pp. 211-244, June 2001.

[13] D. G. Tzikas, A. C. Likas, and N. P. Galatsanos, "The variational approximation for Bayesian inference," *IEEE Signal Process. Mag.*, vol. 25, no. 6, pp. 131-146, Nov. 2008.

[14] P. Chen, Y. Rong, and S. Nordholm, "Variational Bayesian channel tracking in high-speed underwater acoustic communication," in *Proc. WUWNet 2015*, Washington, DC, USA, Oct. 22-24, 2015.

[15] G. Ndo, P. Siohan, and M.-H. Hamon, "Adaptive noise mitigation in impulsive environment: Application to power-line communications," *IEEE Trans. Power Delivery*, vol. 25, pp. 647-656, Apr. 2010.

[16] P. Chen, Y. Rong, S. Nordholm, and Z. He, "Joint channel and impulsive noise estimation in underwater acoustic OFDM systems," *IEEE Trans. Veh. Technol.*, vol. 66, pp. 10567-10571, Nov. 2017.